Article

Journal of
Nanoscience and Nanotechnology
Vol. 15, 8388–8394, 2015
www.aspbs.com/jnn

Synthesis of $CuIn_{1-x}Ga_xSe_2$ Nanoparticles by Thermal Decomposition Method with Tunable Ga Content

M. Latha[1], R. Aruna Devi[1], S. Velumani[1,2,3,*], Goldie Oza[2], P. Reyes-Figueroa[2], M. Rohini[2], I. G. Becerril-Juarez[1], and Junsin Yi[3,*]

[1] *Program on Nanoscience and Nanotechnology;* [2] *Department of Electrical Engineering (SEES), CINVESTAV-IPN, Avenida IPN 2508, San Pedro Zacatenco, Mexico, D.F*
[3] *School of Information and Communication Engineering, Sungkyunkwan University, 300 Cheoncheon-Dong, Jangan-Gu, Suwon, 440-746, Korea*

Chalcopyrite $CuIn_{1-x}Ga_xSe_2$ (CIGS) nanoparticles were synthesized by mixing copper (I) chloride (CuCl), Indium (III) chloride ($InCl_3$), gallium (III) chloride ($GaCl_3$) and selenium (Se) in oleylamine (OLA) at 260 °C for 4 h under nitrogen atmosphere. The Ga/(In + Ga) ratio was tuned across the entire stoichiometric range from 0 to 1. X-ray diffraction analysis (XRD) revealed chalcopyrite crystal structure for samples prepared with $x = 0$, 0.3, 0.5, 0.7 and 1. The lattice parameters a and c decreased linearly with increasing Ga concentration which is consistent with Vegard's law. Raman spectra exhibited A_1 optical phonon vibrational mode for synthesized nanoparticles which gradually shifted to higher wavenumber with increasing Ga content. Field emission scanning electron microscopy (FE-SEM) and transmission electron microscopy (TEM) images showed irregular as well as hexagonal plate like morphologies in the size range of 100 to 400 nm. High-resolution transmission electron microscopy (HR-TEM) images showed well-defined lattice fringes and d-spacing correspond to (112) plane which gradually decreases with increasing Ga content. The material compositions of synthesized CIGS nanoparticles with $x = 0$, 0.3, 0.5, 0.7 and 1 were very close to the desired stoichiometry which was confirmed by energy dispersive X-ray analysis (EDAX). Ultraviolet visible near infrared (UV-VIS-NIR) absorption spectra of the synthesized CIGS nanoparticles revealed that the bandgap could be tuned over the range 1 to 1.7 eV by varying the Ga/(In+Ga) ratio.

Keywords: $CuIn_{1-x}Ga_xSe_2$, Chalcopyrite, Thermal Decomposition.

1. INTRODUCTION

With increasing global energy consumption, there is a need to search for an alternative renewable energy using natural resources. Amongst them, solar energy has been widely employed using photovoltaic (PV) which can harvest and directly convert solar energy into electricity.[1] In the past two decades, various semiconducting nanomaterials have been used to fabricate PV devices such as CdTe,[2] PbSe,[3] $CuInSe_2$,[4] $CuIn_xGa_{1-x}Se_2$[5] and $Cu_2ZnSnSe_4$.[6] In particular, $CuIn_xGa_{1-x}Se_2$ (CIGS) has been studied extensively as an absorber material in solar cells because of high absorption coefficient ($\alpha \sim 10^5$ cm^{-1}), good photostability and direct band gap which is tunable from 1 to 1.7 eV by varying Ga/(In + Ga) ratio.[7,8] To date, CIGS solar cell efficiency as high as 20.4% has been demonstrated with $Eg = 1.2$ eV.[9]

In recent years, vacuum based techniques such as co-evaporation[10] and sputtering[11] have been considered to be the best to produce high quality CIGS thin films. In contrary, these techniques are expensive[12] and causes more wastage of materials during the course of deposition.[13,14] Due to these obstacles, solution based techniques have been developed to make CIGS thin film which usually involves the deposition either by solution or nanoparticle precursors. The thin film deposition by nanoparticle precursors offers the advantage of an easy synthesis process. Until now, several techniques have been devolped for the synthesis of CIGS nanoparticles

*Authors to whom correspondence should be addressed.

 1533-4880/2015/15/8388/007 doi:10.1166/jnn.2015.11473

including hydrothermal/solvothermal technique,[15] ball milling technique,[16] hot injection method[17] and thermal decomposition method[18] etc.

In this work, we report a facile and inexpensive thermal decomposition method for synthesizing CIGS nanoparticles. This is a unique study which involves the gradual refluxing of metal precursors in oleylamine by varying temperature from 140 °C to 260 °C for obtaining single-phase CIGS nanoparticles. The synthesized nanoparticles possess good trends in their lattice constants (a and c) variation when they were modulated by their x values. Structural, morphological and compositional studies showed the effect of Ga content when Ga/(In + Ga) concentration was varied from 0 to 1. We demonstrate for the first time, mechanism for the formation of CIGS using thermal decomposition method, which involves phase transformation from β-CuSe to CIGS with increase in the temperature. In future, these synthesized nanoparticles can be used to prepare ink for the deposition of CIGS thin films.

2. EXPERIMENTAL DETAILS

Copper (I) chloride (CuCl; 99.995%), indium (III) chloride ($InCl_3$; anhydrous 99.999%), gallium (III) chloride ($GaCl_3$; anhydrous 99.999%), elemental selenium (Se; 99.99%), oleylamine (OLA; technical grade 70%), absolute ethanol and chloroform (99.99%) were purchased from Sigma-Aldrich. All chemicals were used without further purification.

A typical reaction was initiated by dissolving 1 mmol of CuCl (0.10 g), 2 mmol of elemental Se (0.16 g) and 1 mmol of $InCl_3$ (0.00 to 0.22 g) & $GaCl_3$ (0.00 to 0.11 g) in 10 ml of OLA to a 50 ml three-neck flask. The composition of $CuIn_{1-x}Ga_xSe_2$ was tuned over entire stoichiometric range with x values of 0, 0.3, 0.5, 0.7 and 1 by adjusting the proportion of Ga and In reactant ratio. The mixture was purged with oxygen and water followed by bubbling nitrogen at 140 °C for 1 h with constant stirring. Next, the temperature of the mixture was increased to 210 °C for 1 h and then heated to 260 °C for 4 h under vigorous stirring. After 4 h, the mixture was cooled to 100 °C and 10 ml of chloroform was added to quench the reaction, 5 ml of ethanol was then added to precipitate the nanoparticles. After ethanol addition, the mixture was immediately centrifuged at 4000 rpm for 20 min. The nanoparticles were dispersed in 10 ml of chloroform and sonicated for 2 min, followed by centrifugation at 4000 rpm for 5 min. This process was repeated three times to get high-purity nanoparticles.

The crystal structure of synthesized nanoparticles were analyzed with X-ray diffractometer (SmartLab, RIGAKU) using Cu-Kα radiation ($\lambda = 1.5406$ Å) source at 45 KV and 200 mA. Micro Raman spectra of synthesized nanoparticles were detected by HORIBA Jobin Yvan with He–Ne laser (632 nm) at room temperature. The morphologies and sizes of synthesized nanoparticles were observed with FE-SEM (Auriga 3916, Carl Zeiss), and the chemical composition was measured with EDAX (XFlash Detector 5010). Furthermore, the morphology of the synthesized nanoparticles were confirmed with HR-TEM (JEM-ARM200F). For HR-TEM analysis, the nanoparticles were dispersed in isopropanol and dried on nickel grid. The bandgap of the synthesized nanoparticles was calculated using absorption spectra which was measured using UV-VIS-NIR spectrophotometer (JASCO V-670) at room temperature.

3. RESULTS AND DISCUSSION

Figures 1(a) and (b) shows XRD pattern of synthesized CIGS nanoparticles with varying Ga/(In + Ga) ratios from 0 to 1. The observed (112), (204/220) and (116/312) planes revealed chalcopyrite crystal structure for all the samples. The 2θ value of (112) plane at 26.7° and 27.7° correspond to $CuInSe_2$ (JCPDS 01-087-2265) and $CuGaSe_2$ (JCPDS 01-075-0104) respectively. The peak position of (112) plane for CIGS at $x = 0.3$, 0.5, and 0.7 was located within the region of $CuInSe_2$ to $CuGaSe_2$. In the case of $x = 0.7$, the (204/220) and (116/312) planes exhibited broadening due to the separation of (204) and (220) as well as (116) and (312) diffraction planes respectively.[19] The diffraction peaks gradually shifted to higher 2θ values with increasing Ga content. This is due to the decreased lattice spacing because of the smaller Ga atoms (0.47 Å) substituted for larger In atoms (0.62 Å). This is in good agreement with Li et al.[20]

Lattice parameters a and c for the tetragonal system were calculated using the formula:[21]

$$\frac{1}{d^2} = \frac{h^2 + k^2}{a^2} + \frac{l^2}{c^2} \quad (1)$$

where, d is the atomic lattice spacing, h, k and l are miller indices, a and c are lattice parameters of the crystal. Figure 2 shows decreased lattice parameters a and c with increasing Ga content. This is in good agreement with Vegard's law which states that lattice parameters decreases linearly with increasing Ga content.[22] The diffraction peaks are shifted to higher 2θ values and lattice parameters a and c were decreased which confirms the variation in Ga content.

The formation mechanism of CIGS nanoparticles using thermal decomposition method was shown in Scheme 1. This could be divided into three-step process. In the first step, the formation of β-CuSe phase was obtained. The dissolution and reduction of elemental Se by OLA forms Se_x^{2-} ions, while, from Cu^+ ions are released from the decomposition of CuCl with OLA. This leads to the formation of β-CuSe which was confirmed by XRD pattern (Fig. 3).[23] This is due to the reactivity of soft base (Se_x^{2-}) with soft acid (Cu^+) rather than hard acids (Ga^{3+} and In^{3+}) at low temperature (i.e., 140 °C). In the second step, Ga^{3+} and In^{3+} ions are released, which are incorporated into the

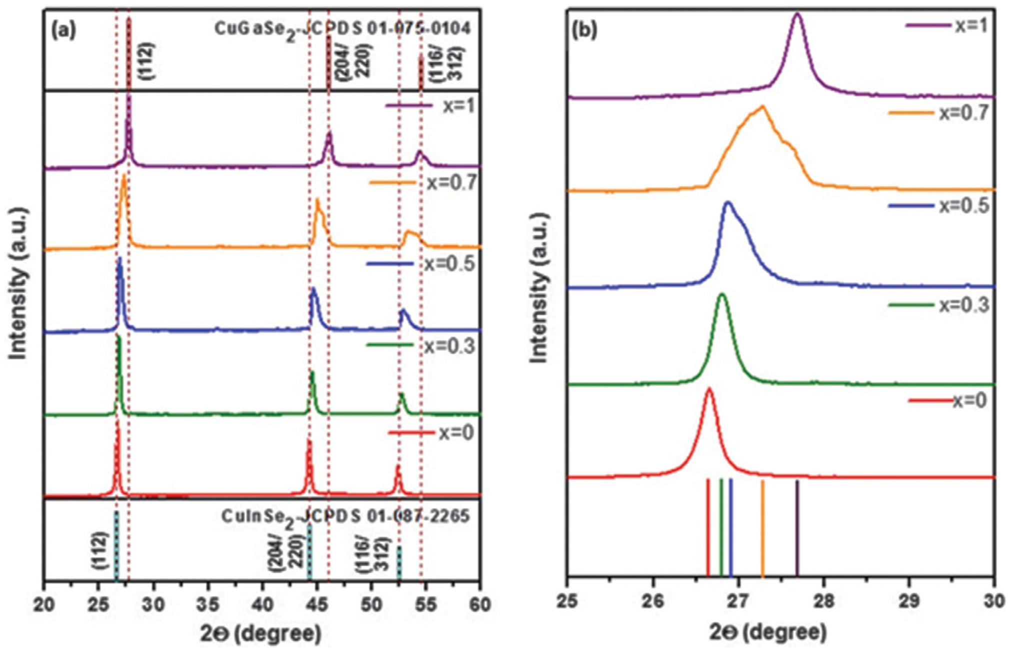

Figure 1. (a) XRD patterns of CIGS nanoparticles with $x = 0$, 0.3, 0.5, 0.7 & 1 and (b) Magnification of the (112) planes.

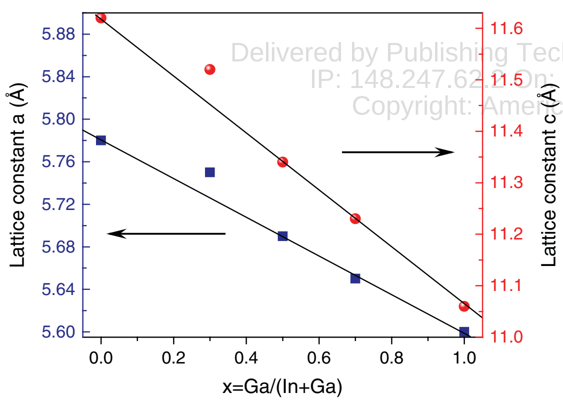

Figure 2. Changes in lattice constants a and c with varying x from 0 to 1.

β-CuSe crystal lattice, resulting in a partial formation of CIGS. A mixed phase of CIGS and β-CuSe were observed in XRD pattern (Fig. 3), where the (112) peak was splitted into two, corresponding to CIGS and β-CuSe at 210 °C. Finally, as the temperature is raised to 260 °C, the release of Ga^{3+} and In^{3+} ions were increased, thus leading to the formation of single phase CIGS. The observed high intense (112), (204/220) and (116/312) peaks along with (103), (211) and (213) less intense peaks correspond to chalcopyrite structure.

Raman spectroscopy was used for further confirmation of Ga effect as shown in Figure 4. All the samples showed the prominent peak corresponding to the A_1 optical phonon vibrational mode of chalcopyrite crystal structure.[24] This peak was originated from pure

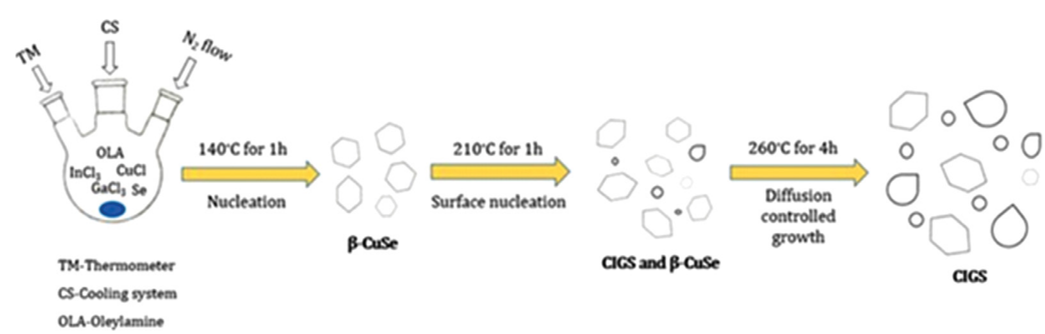

Scheme 1. CIGS nanoparticles synthesis via thermal decomposition.

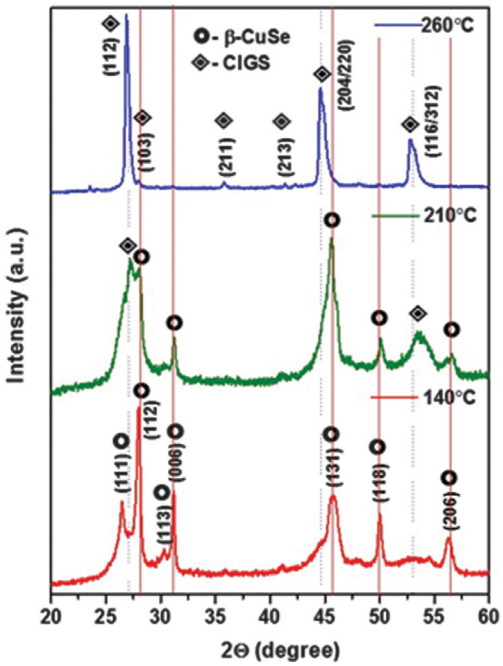

Figure 3. XRD patterns of CIGS nanoparticles synthesized at various reaction temperature (140 °C, 210 °C and 260 °C).

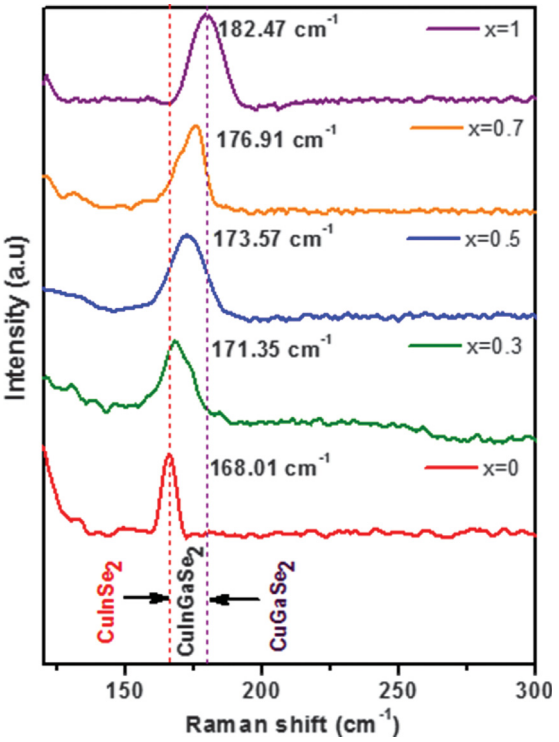

Figure 4. Raman spectra of CIGS nanoparticles with $x = 0$, 0.3, 0.5, 0.7, and 1.

anionic (Se) mode vibrations regardless of static neighboring cations (Cu, In and Ga). A_1 peaks at 168.01 and 182.47 cm^{-1} correspond to $CuInSe_2$ and $CuGaSe_2$ respectively. A_1 peak positions of CIGS at $x = 0.3$, 0.5, and 0.7 were within the range of 168.01 to 182.47 cm^{-1}. As Ga content increases, the peak position is shifted to higher wavenumber. The same behavior was found by Olejnicek et al.[19]

Figures 5(a)–(e) shows FE-SEM micrographs of the synthesized CIGS nanoparticles with varying x values from 0 to 1. The morphology of the particles were irregular as well as hexagonal plate like shapes with in the size range of 100 to 400 nm including some seed plates in the size range of 10 to 100 nm for all the samples (Figs. 5(a)–(e)). The inhomogeneous size distribution and irregular shape of particles are due to the "digestive ripening" which causes rearrangement of nanoparticles at higher temperature for longer reaction time.[25,26] The EDAX spectrum of CIGS nanoparticles synthesized with $x = 0$, 0.3, 0.5, 0.7 and 1 were shown in Figures 5(f)–(j). The material composition of CIGS with x from 0 to 1 is very close to the desired stoichiometry.

Figures 6(a)–(e) shows TEM micrographs of the synthesized CIGS nanoparticles with varying x values from 0 to 1. For all the cases, the morphology of the particles were irregular as well as hexagonal plate like shapes with in the size range from 200 to 400 nm as observed in FE-SEM micrographs. Fast Fourier Transform (FFT) (inset) was calculated using HR-TEM images (Figs. 6(f)–(j)) and they showed well-defined lattice fringes with the d-spacing values of 0.333 nm, 0.330 nm, 0.327 nm, 0.326 nm and 0.321 nm which is assigned to (112) lattice plane of tetragonal chalcopyrites $CuInSe_2$, $CuIn_{0.7}Ga_{0.3}Se_2$, $CuIn_{0.5}Ga_{0.5}Se_2$, $CuIn_{0.3}Ga_{0.7}Se_2$ and $CuGaSe_2$, respectively.[20] Therefore, there is a gradual decrement in the lattice spacing of d(112) with increasing Ga content, this is in good agreement with the d-spacing values from the XRD patterns.

Figure 7(a) shows the UV-VIS-NIR absorption spectra of the synthesized CIGS nanoparticles with varying Ga/(In + Ga) ratio from 0 to 1, which were measured after dispersing in toluene. From the spectra, it is clear that the absorption started at the near infrared region and it rises gradually in the UV-Visible region. The same behaviour was observed from many other nanocrystals.[18,27] Meanwhile, there is blue shift towards shorter wavelength with increasing Ga content. The Tauc relationship is used to calculate the optical bandgap energy of synthesized nanoparticles by extrapolating $(\alpha h\nu)^2$ versus $h\nu$ as shown in Figure 7(b). The bandgap of the synthesized nanoparticles for $x = 0$, 0.3, 0.5, 0.7 and 1 are found to be 1.07 eV, 1.22 eV, 1.38 eV, 1.5 eV and 1.66 eV respectively. The measured bandgap values are in good agreement with

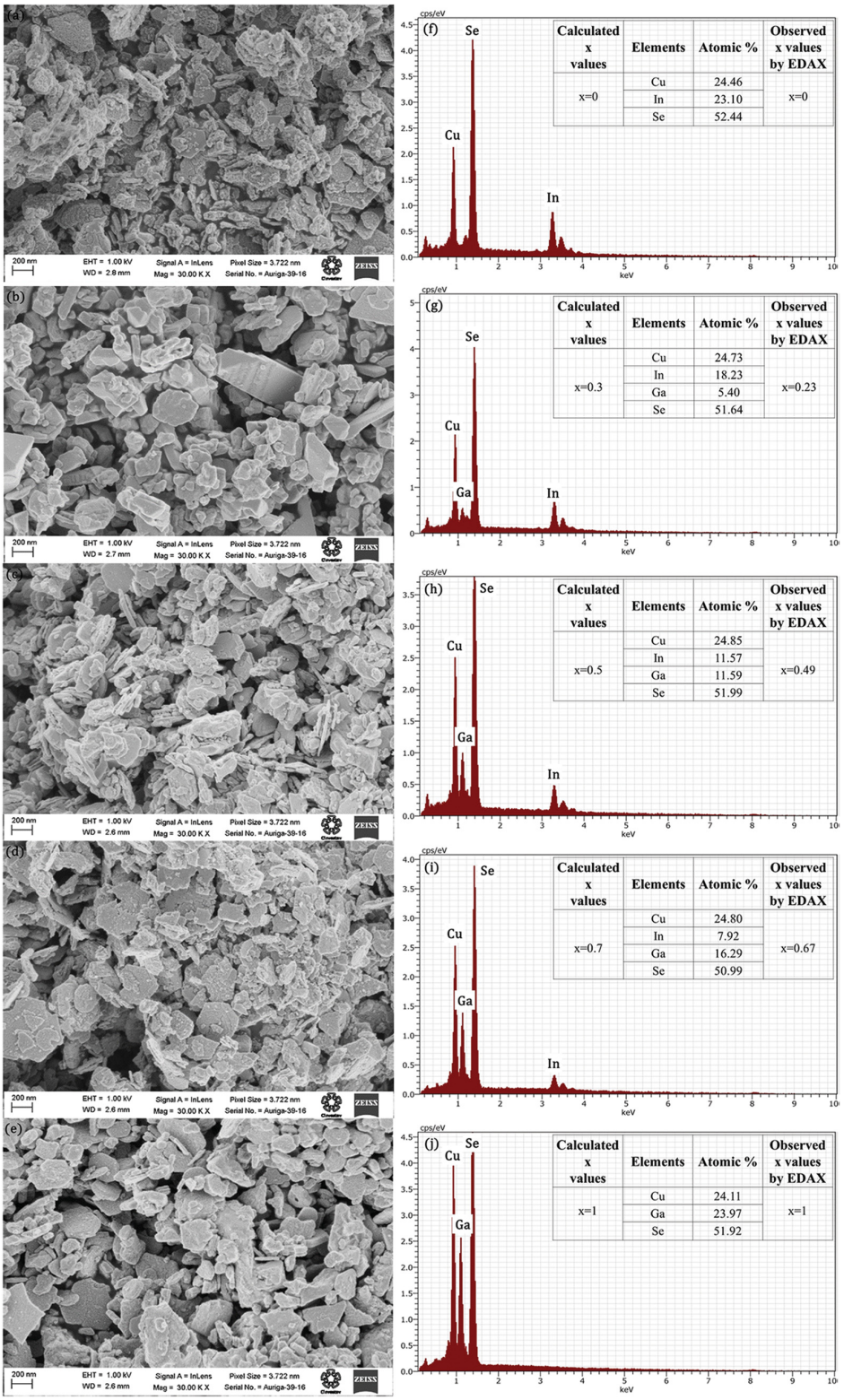

Figure 5. FE-SEM images and EDAX spectrums of the nanoparticles synthesized with Ga/(In + Ga) ratio where (a), (f) $x = 0$, (b), (g) $x = 0.3$, (c), (h) $x = 0.5$, (d), (i) $x = 0.7$ and (e), (j) $x = 1$.

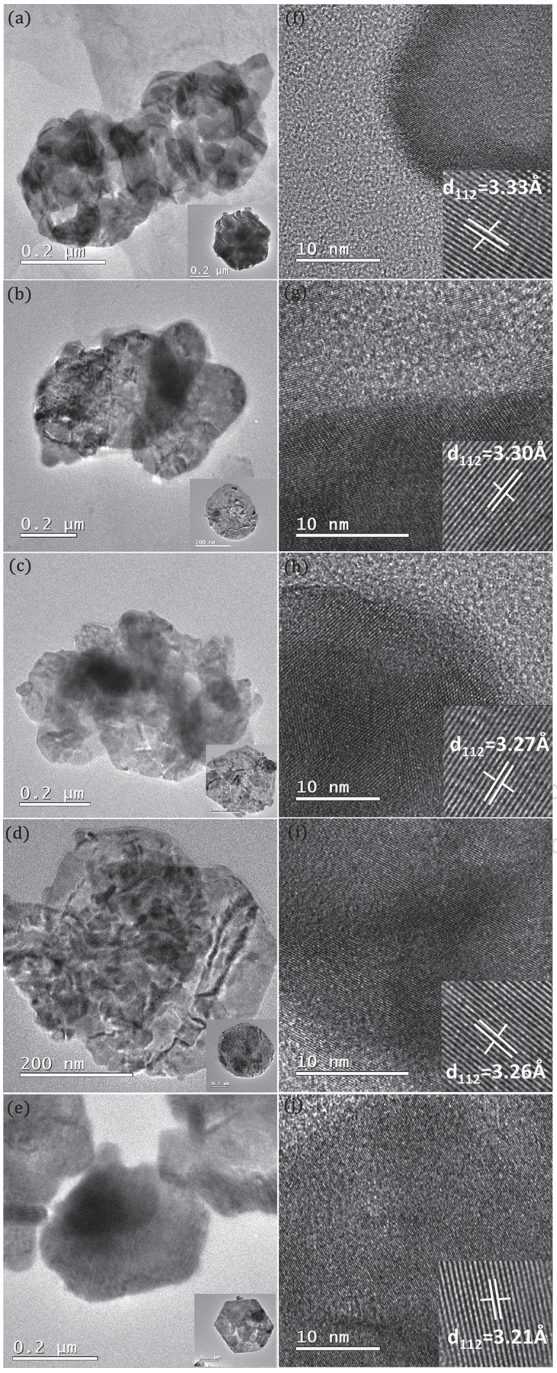

Figure 6. TEM and HR-TEM images of the nanoparticles synthesized with varying Ga/(In + Ga) ratio where (a), (f) $x = 0$, (b), (g) $x = 0.3$, (c), (h) $x = 0.5$, (d), (i) $x = 0.7$ and (e), (j) $x = 1$. The inset (f)–(j) shows the lattice fringe distance.

calculated values by bowing equation.[20] Therefore, the obtained results indicate that the bandgap can be tuned by simply adjusting Ga/(In + Ga) ratio in the thermal decomposition method.

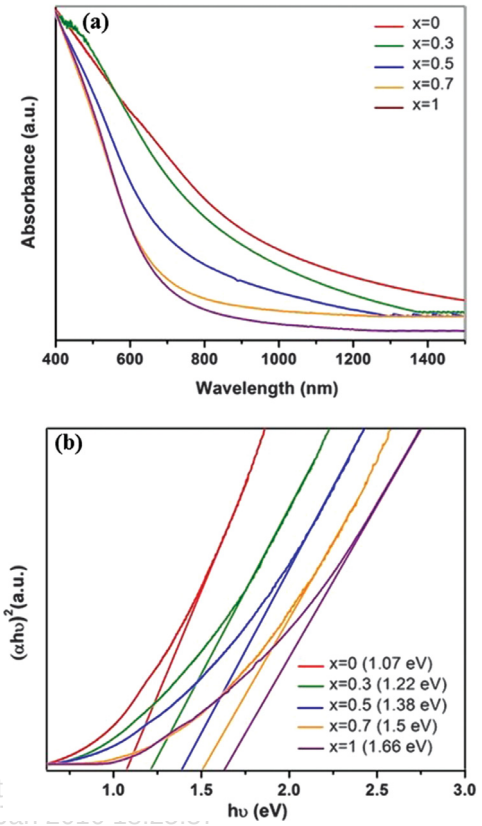

Figure 7. (a) UV-VIS-NIR absorption spectra of synthesized CIGS nanoparticles with $x = 0$ to 1 and (b) the corresponding plot of $(\alpha h\nu)^2$ versus $(h\nu)$.

4. CONCLUSION

In this work, we have synthesized CIGS nanoparticles with different Ga content using thermal decomposition of metal-chlorides and selenium. The synthesized CIGS nanoparticles revealed chalcopyrite crystal structure. Lattice parameters a and c were found to be decreased with increasing Ga content which is in accordance with Vegard's law. A_1 vibrational mode is shifted to higher wavenumber with increasing Ga content. Irregular and hexagonal plate-like particles were observed and in the size range of 100 to 400 nm. Chemical composition of CIGS at $x = 0$, 0.3, 0.5, 0.7 and 1 were close to the desired stoichiometry. The d-spacing of (112) plane gradually decreased with increasing Ga content. The bandgap of the synthesized CIGS nanoparticles proves that it is tunable in the range of 1 to 1.7 eV by varying Ga/(In + Ga) ratio. The synthesized CIGS nanoparticles will be used to prepare ink for the deposition of CIGS thin films, which can be employed for solar cell fabrication.

Acknowledgments: The authors are grateful for the funding from ICyT through project 326/11. We wish to acknowledge Alvaro Angeles Pascual (HR-TEM),

Josue E. Romero Ibarra (FE-SEM-EDAX), Marcela Guerrero (XRD) and Alejandra Garcia-Sotelo (Raman) for their technical support. We thank the partial financial support from the projects CeMIE-Sol 207450/P26 and from Human Resource Development Program grant (No. 20124010203280) of the Korea Institute of Energy Technology Evaluation and Planning (KETEP) funded by the Ministry of Trade, Industry and Energy of the Korean government. One of the co-authors (SV) is thankful for the support from MSIP (Ministry of Science, Ict and future Planning)-(141S-6-3-0641), South Korea.

References and Notes

1. S. Chu and A. Majumdar, *Nature* 488, 294 (**2012**).
2. J. Jasieniak, B. I. MacDonald, S. E. Watkins, and P. Mulvaney, *Nano Lett.* 11, 2856 (**2011**).
3. J. J. Choi, Y. F. Lim, M. B. Santiago-Berrios, M. Oh, B. R. Hyun, L. Sun, A. C. Bartnik, A. Goedhart, G. G. Malliaras, H. D. Abruna, F. W. Wise, and T. Hanrath, *Nano Lett.* 9, 3749 (**2009**).
4. W. Wang, Z. Jin, H. Liu, and H. Du, *Mater. Lett.* 65, 2895 (**2011**).
5. J. H. Lee, J. Chang, J. H. Cha, Y. Lee, J. E. Han, D. Y. Jung, E. C. Choi, and B. Hong, *Eur. J. Inorg. Chem.* 2011, 647 (**2011**).
6. C. Steinhagen, M. G. Panthani, V. Akhavan, B. Goodfellow, B. Koo, and B. A. Korgel, *J. Am. Chem. Soc.* 131, 12554 (**2009**).
7. V. A. Akhavan, T. B. Harvey, C. J. Stolle, D. P. Ostrowski, M. S. Glaz, B. W. Goodfellow, M. G. Panthani, D. K. Reid, D. A. V. Bout, and B. A. Korgel, *ChemSusChem.* 6, 481 (**2013**).
8. J. Tang, S. Hinds, S. O. Kelley, and E. H. Sargent, *Chem. Mater.* 20, 6906 (**2008**).
9. A. Chirilă, P. Reinhard, F. Pianezzi, P. Bloesch, A. R. Uhl, C. Fella, L. Kranz, D. Keller, C. Gretener, H. Hagendorfer, D. Jaeger, R. Erni, S. Nishiwaki, S. Buecheler, and A. N. Tiwari, *Nat. Mater.* 12, 1107 (**2013**).
10. K. Ramanathan, M. A. Contreras, C. L. Perkins, S. Asher, and F. S. Hasoon, *Prog. Photovolt. Res. Appl.* 11, 225 (**2003**).
11. J. Liu, D. Zhuang, H. Luan, M. Cao, and M. Xie, *Progress in Natural Science* 23, 133 (**2013**).
12. C. Eberspacher, C. Fredric, K. Pauls, and J.Serra, *Thin solid Films* 387, 18 (**2001**).
13. T. Wada, H. Kinoshita, and S. Kawata, *Thin Solid Films* 431–432, 11 (**2003**).
14. Y. Liu, D. Kong, H. You, C. Zhao, and J. Li, *Electrochem. Solid-State* 1, 26 (**2012**).
15. B. Li, Y. Xie, J. Huang, and Y. Qian, *Adv. Mater.* 11, 1456 (**2009**).
16. B. Vidya, S. Velumani, J. A. Arenas-Alatorre, A. M. Acevedo, R. Asomoza, and J. A. Chavez-Carvayar, *Mater. Sci. Eng. B* 174, 216 (**2010**).
17. M. Ahmadi, S. S. Pramana, L. Xi, C. Boothroyd, Y. M. Lam, and S. Mhaisalkar, *J. Phys. Chem. C* 116, 8202 (**2012**).
18. M. G. Panthani, V. Akhavan, B. Goodfellow, J. P. Schmidtke, L. Dunn, A. Dodabala-pur, P. F. Barbara, and B. A. Korgel, *J. Am. Chem. Soc.* 130, 16770 (**2008**).
19. J. Olejnıček, C. A. Kamler, A. Mirasano, A. L. Martinez-Skinner, M. A. Ingersoll, C. L. Exstroma, S. A. Darveau, J. L. Huguenin-Love, M. Diaz, N. J. Ianno, and R. J. Soukup, *Solar Energy Materials and Solar Cells* 94, 8 (**2010**).
20. J. Li, Z. Jin, T. Liu, J. Wang, D. Wang, J. Lai, H. Dub, and L. Cuib, *CrystEngComm.* 15, 7327 (**2013**).
21. D. Lee, S. Park, and J. H. Kim, *Current Applied Physics* 11, S88 (**2011**).
22. S. N. Malik, S. Mahboob, N. Haider, M. A. Malika, and P. O'Brien, *Nanoscale* 3, 5132 (**2011**).
23. W. H. Hsu, H. I. Hsiang, Y. L. Chang, D. T. Ray, and F. S. Yen, *J. Am. Ceramic. Soc.* 94, 3030 (**2013**).
24. A. Chirilă, S. Seyrling, S. Buecheler, D. Guettler, S. Nishiwaki, Y. E. Romanyuk, G. Bilger, and A. N. Tiwari, *Prog. Photovolt: Res. Appl.* 20, 209 (**2012**).
25. S. I. Stoeva, K. J. Klabunde, C. M. Sorensen, and I. Dragieva, *J. Am. Chem. Soc.* 124, 2305 (**2002**).
26. J. Park, J. Joo, S. G. Kwon, Y. Jang, and T. Hyeon, *Angew. Chem. Int. Ed.* 46, 4630 (**2007**).
27. M. Y. Chiang, S. H. Chang, C. Y. Chen, F. W. Yuan, and H. Y. Tuan, *J. Phys. Chem. C* 115, 1592 (**2011**).

Received: 17 August 2014. Accepted: 5 March 2015.